

## Visibility parameterization from microphysical observations for warm fog conditions and its application to the Canadian MC2 model

P3.7

I. Gultepe, J. Milbrandt<sup>2</sup>, and S. Belair<sup>2</sup>

<sup>1</sup>Environment Canada, Cloud Physics and Severe Weather Research Division  
Toronto, ON M3H5T4, Canada

<sup>2</sup>Meteorological Services of Canada,  
RPN, Dorval, QC, Canada

### 1. INTRODUCTION

Fog formation is directly related to thermodynamical, dynamical, radiative, aerosol, and microphysical processes, and surface conditions. Extinction of light at visible ranges within the fog results in low visibilities that can affect low-level flight conditions, marine traveling, shipping, and transportation. Fog occurrence more than 10% of time in some regions of Canada (Whiffen, 2001) demands that fog nowcasting and/or forecasting models should be improved. Particularly, fog intensity, represented with visibility ( $Vis$ ), should be more accurately simulated to reduce the costs of fog-related accidents and to delays at airports and in marine environments, and accidents.

The earlier studies on  $N_d$  and  $LWC$  relationships showed that there is usually a large variability on  $N_d$  for a given  $LWC$  (Gultepe et al., 2001; Gultepe and Isaac, 2004a). The work by Gultepe and Isaac (2004b) on fog microphysics suggested that  $N_d$  can change from a few droplets per volume to  $100 \text{ cm}^{-3}$  for a fixed  $LWC$  and that visibility should be function of both  $N_d$  and  $LWC$ . These works indicated that  $N_d$  should be considered in visibility parameterizations. Previously, Bott and Trautmann (2002), using prognostic equations, developed a model that predicted both total number concentration ( $N_d$ ) and  $LWC$ . Under the saturated conditions, more cloud concentration nuclei ( $CCN$ ) leads to the formation of a large number of small droplets (Gultepe and Isaac, 1999), resulting in slower gravitational settling of droplets and thus low visibility. As shown by the experimental relation of Jiusto (1981), visibility is directly

Related to average cloud droplet radius (hence number concentration) that is indirectly related to  $LWC$ . This shows that visibility parameterizations should also include number concentration of droplets as an independent variable.

In the present work, a new parameterization scheme for warm fog visibility as function of both liquid water content ( $LWC$ ) and droplet number concentration ( $N_d$ ) is suggested and compared with the results of earlier studies. Then, applying the new parameterization, the Canadian Mesoscale Cloud (MC2) model (Benoit et al., 1997) is used to obtain  $Vis$  values for a case study.

### 2. OBSERVATIONS

Observations used to develop new microphysical parameterization for warm fog were collected during the Radiation and Aerosol Cloud Experiment (RACE), representing boundary layer low level clouds (Gultepe et al., 2001), that took place over Eastern Canada during the months of August and October in 1995. During the field program, some low-level clouds with base heights lower than 100 m height occurred. Although fog was also observed over the Atlantic Ocean, observations were limited to higher levels within the clouds because of flight restrictions.

The main in-situ measurements such as  $N_d$  and droplet size, aerosol number concentrations ( $N_a$ ),  $LWC$ , temperature ( $T$ ), and relative humidity ( $RH_v$ ) were collected by the Forward Scattering Spectrometer Probe (FSSP), Particle Cavity Axial Spectrometer Probe (PCASP), hot wire probes (e.g. King Probe), Rosemount T probe, and EG&G dew point hygrometer, respectively, over 16 flights that represented low level clouds with various air mass origins.  $N_d$  was obtained using the FSSP-100 with original size range (2.1-48.4  $\mu\text{m}$ , FSSP-96) and extended size range (4.6-88.7  $\mu\text{m}$ , FSSP-124). Microphysical parameters such as  $N_d$ ,  $LWC$ , and extinction parameters were directly obtained using

---

<sup>1</sup> Corresponding author address: Ismail Gultepe, Environment Canada, Cloud Physics and Severe Weather Research Division, Toronto, ON M3H5T4, Canada, [ismail.gultepe@ec.gc.ca](mailto:ismail.gultepe@ec.gc.ca)

in-situ observations collected along constant altitude flight legs and aircraft profiles. In order to represent important scales related to fog formation, measurements were averaged over 1 km scale. Additional information on observations can be found in Gultepe et al. (1996).

### 3.PARAMETERIZATION AND RESULTS

Using the in-situ observations collected during RACE,  $LWC$ ,  $N_d$ , and the extinction parameter ( $\beta_{ext}$ ) are used to obtain a relationship between visibility ( $Vis$ ) and  $N_d$ , and  $LWC$ , and then  $Vis=f(LWC,N_d)$  is derived. The extinction parameter was calculated from FSSP probe measurements as follows,

$$\beta_{ext} = \sum Q_{ext} n(r) \pi r^2 dr, \quad (1)$$

where  $n$  is the number density of particles in a bin size as radius ( $r$ ) and  $Q_{ext}$  is the Mie efficiency factor. For large size parameters, it becomes approximately 2 (Koenig, 1971; Brenguier et al., 2000), and then it is converted to  $Vis$  using an equation given by (Stoelinga and Warner, 1999) as

$$Vis = -\ln(0.02) / \beta_{ext} \quad (2)$$

The new parameterization is developed after showing the relationships between  $Vis$  and  $LWC$ , and between  $Vis$  and  $N_d$ . Fig. 1 shows  $LWC$  obtained from hot-wire probes versus  $N_d$  that is based on FSSP-100. The  $LWC$  increases with increasing  $N_d$  but for a given  $LWC$ ,  $N_d$  changes from a few droplets per volume up to  $100 \text{ cm}^{-3}$ . The fitted lines in Fig.1 for FSSP96 and FSSP124 are given as

$$LWC_{96} = 1 \times 10^{-6} N_d^2 + 0.0014 N_d \quad (3)$$

and

$$LWC_{124} = 3 \times 10^{-7} N_d^2 + 0.0009 N_d, \quad (4)$$

respectively. The fits to the FSSP data show significant differences related to their size ranges; here, the FSSP96 observations were considered in the calculations because of the existence of small fog droplets ( $<50 \mu\text{m}$ ). This size range was also used in Meyer et al. (1984).

Fig. 2 shows  $Vis$  versus  $N_d$  obtained from the FSSP measurements and a fit to 1 km averaged data. This figure also shows that  $Vis$  decreases quickly while  $N_d$  increases for  $N_d < 100 \text{ cm}^{-3}$  and then gradually for  $N_d > 100 \text{ cm}^{-3}$ . The equation for fit is obtained as

$$Vis = 44.989 N_d^{-1.1592}, \quad (5)$$

with a correlation coefficient of  $R=0.85$ . Large changes in  $Vis$  occur when  $N_d$  changes from a few droplets up to  $100 \text{ cm}^{-3}$ . Above  $100 \text{ cm}^{-3}$ ,  $Vis$  becomes less than 100 m. The large value of  $R$  and less scattering around the fit clearly indicates that  $Vis$  is a strong function of  $N_d$ . Figs. 3a and 3b show a heavy fog case and clear air case, respectively, indicating importance of droplet number concentration effect on visibility.

Fig. 4 shows both  $Vis$  versus  $LWC$  and  $Vis$  versus ice water content ( $IWC$ ) for reference. It is seen that variability in  $Vis$  as a function of condensed water content is comparable to variability in  $Vis$  as a function of  $N_d$  shown earlier. The fit for  $Vis$  ( $Vis_{obs}$ ) versus  $LWC$  is obtained as

$$Vis_{obs} = 0.0219 LWC^{-0.9603}. \quad (6)$$

The  $Vis_{obs}$  (Fig. 4) becomes smaller at  $LWC > 0.03 \text{ g m}^{-3}$  compared to the Kunkel (1984) fit ( $Vis_K$ ), and becomes larger at  $LWC < 0.03 \text{ g m}^{-3}$ . The root mean square error (rmse) and mean relative error (mre) in  $Vis$  estimation are estimated to be about 37 m and 44%, respectively.

The  $Vis_K$  parameterization was also based on FSSP measurements in the size range of 0.5 to  $45 \mu\text{m}$ . The parameterizations for extinction coefficient versus  $LWC$  from Kunkel (1984) and versus  $IWC$  from Stoelinga and Warner (1999) are given, respectively, as

$$\beta_{ext,water} = 144.7 LWC^{0.88} \quad (7a)$$

and

$$\beta_{ext,ice} = 163.9 IWC^{1.0}, \quad (7b)$$

where  $\beta_{ext}$  and  $LWC$  have units of [ $\text{km}^{-1}$ ] and [ $\text{g m}^{-3}$ ], respectively. Then,  $\beta_{ext}$  from Eq. 7a is converted to  $Vis_K$  using Eq. 2. After conversion,  $Vis_K$  versus  $LWC$  is obtained as

$$Vis_K = 0.027 LWC^{-0.88}. \quad (8)$$

Using information that  $Vis$  decreases with increasing  $N_d$  and  $LWC$  obtained from Figs. 2 and 4, a relationship between  $Vis_{obs}$  and  $(LWC \cdot N_d)^{-1}$  is searched. Then, as described in Gultepe (2004),  $Vis$  is parameterized as a function of both  $N_d$  and  $LWC$  (Fig. 5) because  $Vis$  is also a strong function of  $N_d$ . The power fit to observed visibility versus  $x_{ft}$  (fog index) defined as  $(LWC \cdot N_d)^{-1}$  is obtained as

$$Vis_{ft} = \frac{1.002}{(LWC \cdot N_d)^{0.6473}}. \quad (9)$$

This fit indicates that  $Vis$  is inversely related to both  $LWC$  and  $N_d$ . The rmse and mean relative error in  $Vis$  estimation equal to 37 m and 44%, respectively.

The larger values of  $x_{fi}$  (corresponding to  $Vis > 100$  km) suggest that variability (and also problems in measurements) in  $Vis$  increases with increasing  $x_{fi}$ , and this can be related to uncertainties in the observations at small values of  $LWC < 0.005 \text{ g m}^{-3}$ . The maximum limiting  $LWC$  and  $N_d$  values used in derivation of Eq. 9 are about  $400 \text{ cm}^{-3}$  and  $0.5 \text{ g m}^{-3}$ , respectively. The minimum limiting  $N_d$  and  $LWC$  values are  $1 \text{ cm}^{-3}$  and  $0.005 \text{ g m}^{-3}$ , respectively.

Uncertainty in the current parameterizations of visibility in the operational models can be followed up in Fig. 6. In this figure,  $Vis$  changes from 0.2 km to 2.9 km for a fixed value of  $LWC$  as  $0.02 \text{ g m}^{-3}$ . Using Kunkel (1984) parameterization (Eq. 8), and Eq. 9, the effect of uncertainties in  $N_d$  and  $LWC$  on visibility calculation are summarized in this figure. It shows that if  $N_d$  is not used,  $Vis$  uncertainty reaches more than 75%. This uncertainty is much worse than the uncertainty in  $Vis$  calculated from Eq. 9 that is function of both  $N_d$  and  $LWC$ . In real observations, uncertainty in  $LWC$  and  $N_d$  observations can be about 10% and 30%, respectively. Note that difference between  $Vis_{obs}$  (Eq. 6) and  $Vis_K$  (Eq. 9) is about 15% (at 500 m Vis) at lower  $LWC$  values ( $< 0.01 \text{ g m}^{-3}$ ); therefore, Eq. 6 can be used for replacing  $Vis_K$  parameterization but not for  $Vis_{fi}$  because of its small uncertainty.

## 4. DISCUSSIONS

### 4.1 New parameterization

Earlier studies suggested that visibility is indirectly related to  $N_d$ . Meyer et al. (1980) showed that  $Vis$  is a function of  $N_d$  and changes with fog intensity. The  $Vis$  values calculated from their equations are represented as  $Vis_{ML}$  and  $Vis_{MH}$  for light and heavy fog conditions, respectively. As shown in Fig. 7 that  $Vis_{ML}$  is larger than  $Vis_P$  (representing the present work). In heavy fog conditions,  $Vis_P$  is almost one order of magnitude less than for light fog cases of Meyer et al. (1980). The parameterizations of Meyer et al. (1980) for light and heavy fog are given, respectively, as

$$Vis_{ML} = 120N_d^{-0.77} \text{ for light fog,} \quad (10)$$

and

$$Vis_{MH} = 80N_d^{-0.11} \text{ for heavy fog.} \quad (11)$$

For the present study, a similar relationship is obtained as

$$Vis_P = 44.989N_d^{-1.1592}. \quad (12)$$

It can be seen that visibility in Fig. 7 according to (Eq. 12) decreases much faster than visibilities of

Meyer et al. (1980). These differences can be related to uncertainties in  $N_d$  measurements in earlier studies or to in-situ measurements collected within the low level clouds. Overall, the results indicate that  $N_d$  should be considered in  $Vis$  parameterizations as an independent variable.

A new field program over the Ontario region to develop model parameterizations and validate model simulations and remote sensing retrievals will take place during the Fall to Spring of 2005-06, and this will continue into the 2006-2007 time period over Eastern Canada for marine fog studies. During this field program, extensive measurements of  $N_d$ ,  $LWC$ , and visibility will be made, representing various atmospheric conditions. It is expected that new observations will be very useful for fog related instrument development, for model validation purposes, and for the development of algorithms for remote sensing studies of fog.

### 4.2 MC2 model simulation

The new parameterization (Eq. 9) is applied to MC2 model for a case study that a cold front moved across the Oregon coast on 13-14 Dec 2001. The simulation was done using MC2, nested from analyses to a 4-km grid with the Milbrandt and Yau (2005) microphysics scheme, which predicts both cloud liquid water content ( $LWC$ ) and total number concentration ( $N_d$ ). Results are shown in Figs. 8 and 9. Fig. 8 shows horizontal view of  $Vis$  calculated using the new parameterization (Eq. 9) based on the MC2 model 12-hour forecast valid at 0200 UTC on December 2001. A cross section is taken along the yellow line, and the results are shown in Fig. 9. Dark blue color shows  $Vis < 50$  m. Light blue color shows  $Vis$  between 1 and 5 km. Fig. 9 Cross sections of  $LWC$  (box a),  $N_d$  (box b), and  $Vis$  (box c).  $Vis$  values  $< 200$  m are seen at western edge of the mountain region. In that location,  $LWC \sim 0.2 \text{ g m}^{-3}$ , and  $N_d \sim 40-80 \text{ cm}^{-3}$ . These numbers are comparable with observed values shown in Fig. 6.

### 4.3 Future works

The results suggest that the new visibility parameterization can significantly improve visibility estimates, and additional tests are required using other forecasting models (e.g. US RUC and the Canadian Meteorological Center (CMC) Global Multiscale Model (GEM)) in the near future where  $N_d$  can be diagnostically obtained from environmental conditions e.g. temperature (Gultepe and Isaac, 2004). When  $N_d$  is obtained, Gultepe et al. (2005) stated that the use of new parameterization in a forecast model could improve  $Vis$  values up to 50%.

The Rapid Update Cycle (RUC) model that is used commonly for numerical forecasting in North America, also utilizes the Kunkel (1984) parameterization (Benjamin et al., 2004). In the near future, a new three-moment bulk microphysical scheme developed by Milbrandt and Yau (2005), which includes independent predictive equations for the number concentration, mass content, and spectral dispersion for six different hydrometeor categories, will be tested in the Canadian GEM model whereby the new visibility parameterization can be directly applied. Additional improvements and validations will also be performed based on the new data set that will be gathered during the fog remote sensing and modeling (FRAM) field program.

## 5. CONCLUSIONS

In this work, observations collected within low-level clouds during the RACE field program were used in the analysis of visibility parameterizations. The following conclusions can be drawn from this study:

- The  $N_d$  ranges from a few droplets per  $\text{cm}^{-3}$  up to a few  $100 \text{ cm}^{-3}$  for a given  $LWC$ , which indicates that visibility should be parameterized as a function of both  $N_d$  and  $LWC$ .
- The earlier parameterizations of visibility were developed based only on functions of  $LWC$  alone, and this caused the over/under estimate of the visibility depending on environmental conditions.
- The cloud condensation nuclei (CCN) can be directly related to  $N_a$ , which can be used as an independent variable to estimate the effect of aerosols on fog formation in large-scale models. Presently, aerosol size distribution is fixed for these simulations so  $N_a$  cannot be used directly for  $N_d$  prediction.
- If  $N_d$  is obtained as a function of environmental conditions such as T (Gultepe and Isaac, 2004), more accurate  $Vis$  predictions can be done even with current operational forecast models without a prognostic  $N_d$ . Thus, visibility estimates based on  $N_d$  and  $LWC$  can be obtained from bulk microphysical schemes used in operational forecast models.

## Acknowledgements

Funding for this work was provided by Environment Canada and by the National Search and Rescue Secretariat of Canada. Technical support

for the data collection was provided by both NRC, Ottawa, and MSC Cloud Physics and Severe Weather Research Division, Toronto, Ontario. Author likes to thank to Dr. W. Jacobs, Langen, Germany, for discussions on cloud microphysical parameters versus visibility.

## 6. REFERENCES

- Benjamin, S. G., D. Dévényi, Stephen S. Weygandt, Kevin J. Brundage, John M. Brown, Georg A. Grell, Dongsoo Kim, Barry E. Schwartz, Tatiana G. Smirnova, Tracy Lorraine Smith and Geoffrey S. Manikin. 2004: An Hourly Assimilation–Forecast Cycle: The RUC. *Mon. Wea. Rev.*, **132**, 495–518.
- Benoit, R., J.M. Desgagne, P. Pellerin, S. Pellerin, Y. Chartier, and S. Desjardins, 1997: The Canadian Mc2: A semi-Lagrangian, semi-implicit wideband atmospheric model suited for finescale process studies and simulation. *Mon. Wea. Rev.*, **125**, 2382–2415.
- Bott, A., and T. Trautmann, 2002: PAFOG—a new efficient forecast model of radiation fog and low-level stratiform clouds. *Atmos. Res.*, **64**, 191–203.
- Brenguier, J. L., H. Pawlowska, L. Schuller, R. Preusker, J. Fischer, Y. Fouquart, 2000 : Radiative properties of boundary layer clouds : Droplet effective radius versus number concentration. *J. Atmos. Sci.*, **57**, 803–821.
- Gultepe, I., Isaac, G. A., Leitch, W. R., and Banic, C. M., 1996: Parameterization of marine stratus microphysics based on in-situ observations: Implications for GCMs. *J. Climate*, **9**, 345–357.
- Gultepe, I., and Isaac G. A., 1999: Scale effects on averaging of cloud droplet and aerosol number concentrations: Observations and models. *J. Climate*. **12**, 1268–1279.
- Gultepe, I., G. A. Isaac, and K. Strawbridge, 2001: Variability of cloud microphysical and optical parameters obtained from aircraft and satellite remote sensing during RACE. *Inter. J. Climate*, **21**, 4, 507–525.
- Gultepe, I., and G. A. Isaac, 2004a: An analysis of cloud droplet number concentration ( $N_d$ ) for climate studies: Emphasis on constant  $N_d$ . *Q. J. Royal Met. Soc.*, **130**, Part A, No. 602, 2377.
- Gultepe, I., and G. A. Isaac, 2004b: Microphysical parameterization for mixed phase clouds using in-situ observations. *14<sup>th</sup> International Conference on Clouds and Precipitation*

AMS meeting, Atlanta, January 2006, USA

- (ICCP), Bologna, Italy, 18-23 July 2004. 1326-1329.
- Gultepe, I., 2004: Canadian plans for upcoming fog studies, *COST 722 Expert Meeting*, 15-16 October 2004, Available at <http://cost.cordis.lu/src/home.cfm>. Toulouse, France.
- Gultepe, I., M. D. Müller, and Z. Boybeyi, 2005: A New Warm Fog Parameterization Scheme for Numerical Weather Prediction Models. *J. Appl. Met.* Submitted..
- Justo, J. E., 1981: Fog structure. *Clouds, Their Formation, Optical Properties, and Effects*, P. V. Hobbs and A. Deepak, Eds., Academic Press, 187–239.
- Koenig, L. R., 1971: Numerical experiments pertaining to warm-fog clearing. *Mon. Wea. Rev.*, **9**, 227-241.
- Kunkel, B. A., 1984: Parameterization of droplet terminal velocity and extinction coefficient in fog models. *J. Appl. Meteor.*, **23**, 34-41.
- Meyer, M. B., J. E. Justo, and G. G. Lala, 1980: Measurements of visual range and radiation-fog (haze) microphysics. *J. Atmos. Sci.*, **37**, 622-629.
- Milbrandt, J., and M. K. Yau, 2005: A multi-moment bulk microphysics parameterization. Part II: A proposed three-moment closure and scheme description. *J. Atmos. Sci.*, in press.
- Stoelinga, M. T., and T. T. Warner, 1999: Nonhydrostatic, Mesobeta-scale model simulations of cloud ceiling and visibility for an east coast winter precipitation event. *J. Appl. Meteor.*, **38**, 385-404.
- Whiffen, B., 2001: Fog: Impact on aviation and goals for meteorological prediction. *2<sup>nd</sup> Conference on Fog and Fog Collection*, St. John's Canada, 15-20 July 2001. 525-528.

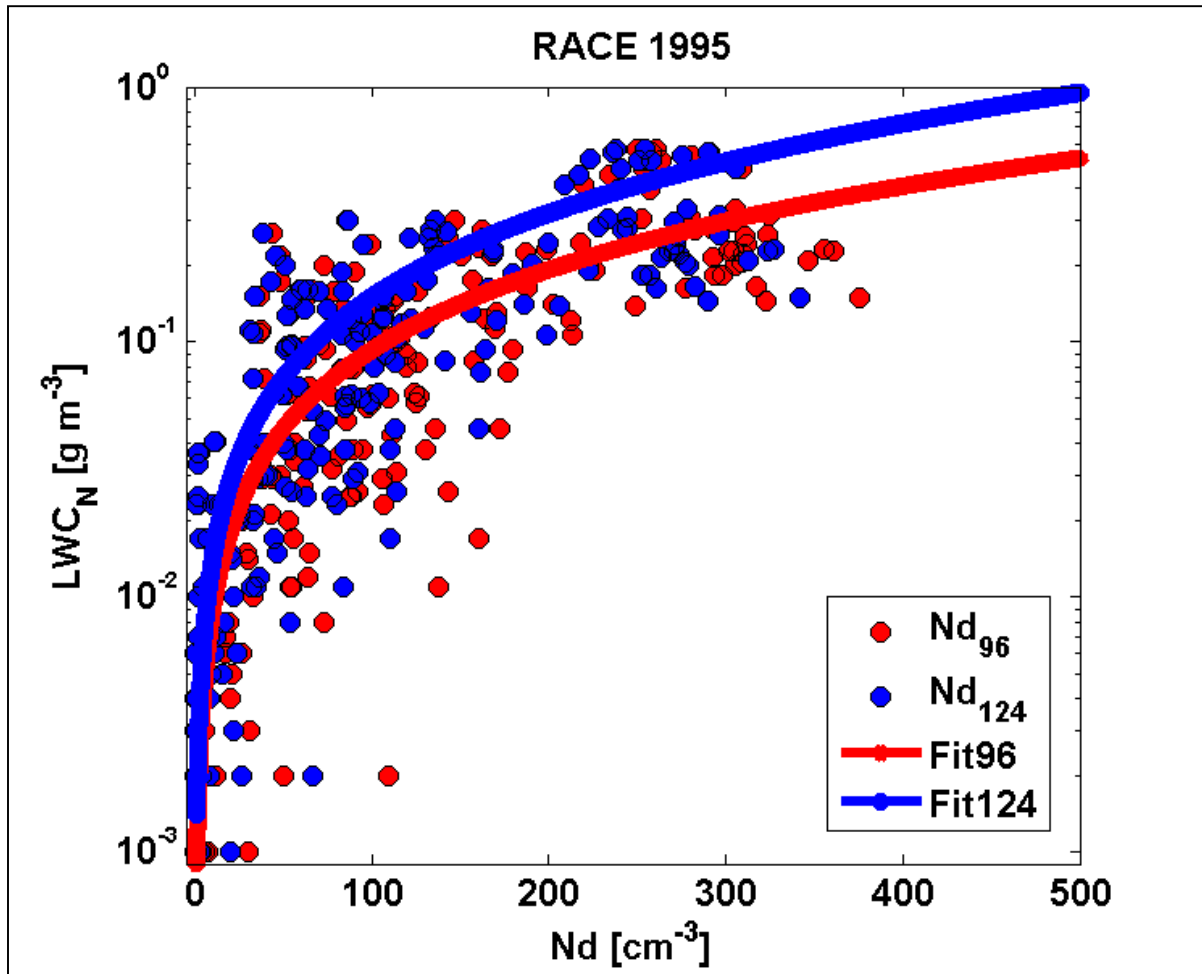


Fig. 1: The  $LWC$  versus  $N_d$  from two FSSP measurements from the RACE field program. Fits are shown by the solid lines. The red and blue filled circles are for FSSP-96 (over original size ranges) and FSSP-124 (over extended size ranges) observations, respectively.

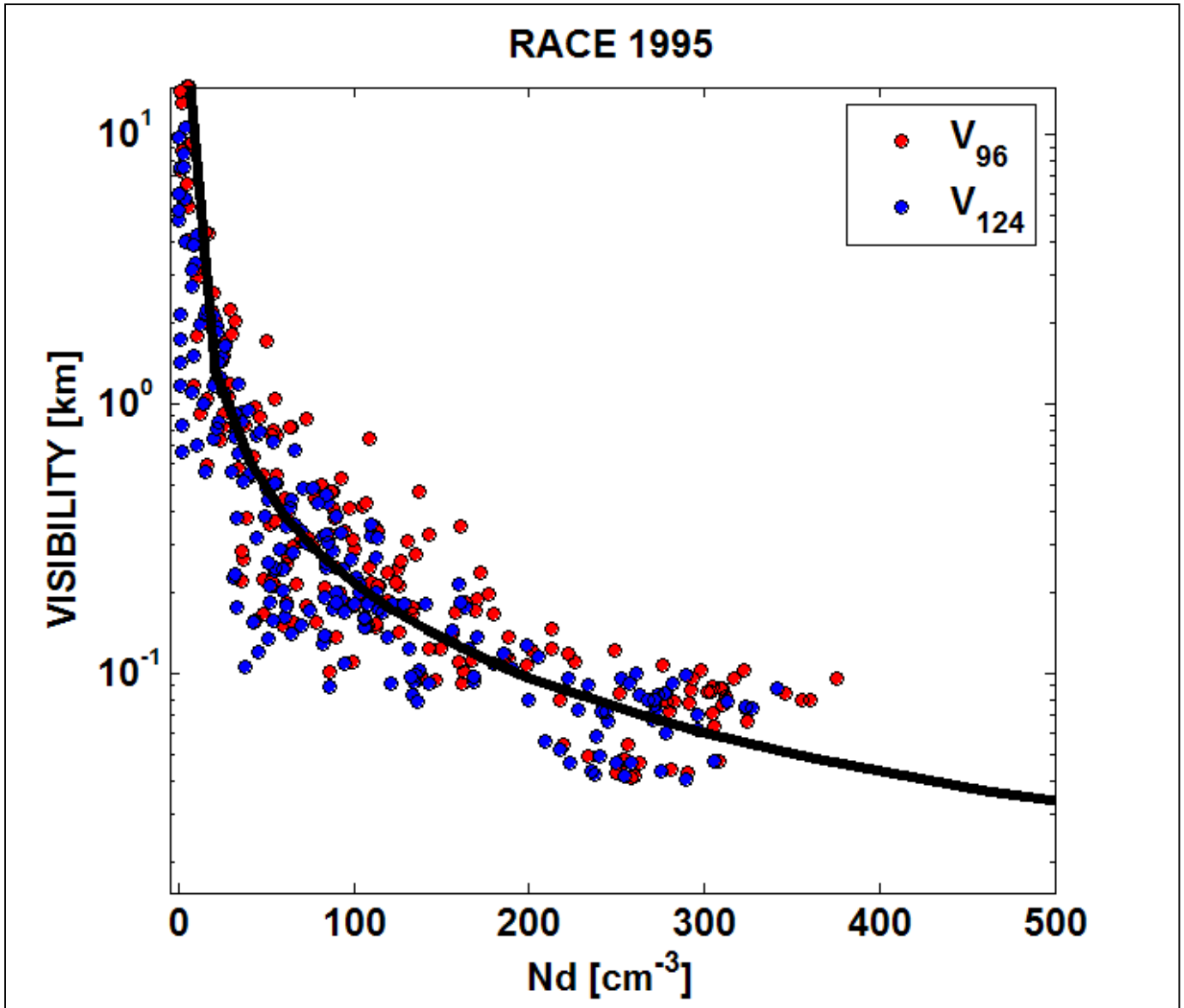


Fig. 2: Visibility versus  $N_d$  from the FSSP measurements, each data point represents a scale of 1 km. The solid fit is for FSSP96. The red and blue filled circles are for FSSP-96 (over original size ranges) and FSSP-124 (over extended size ranges) observations, respectively.

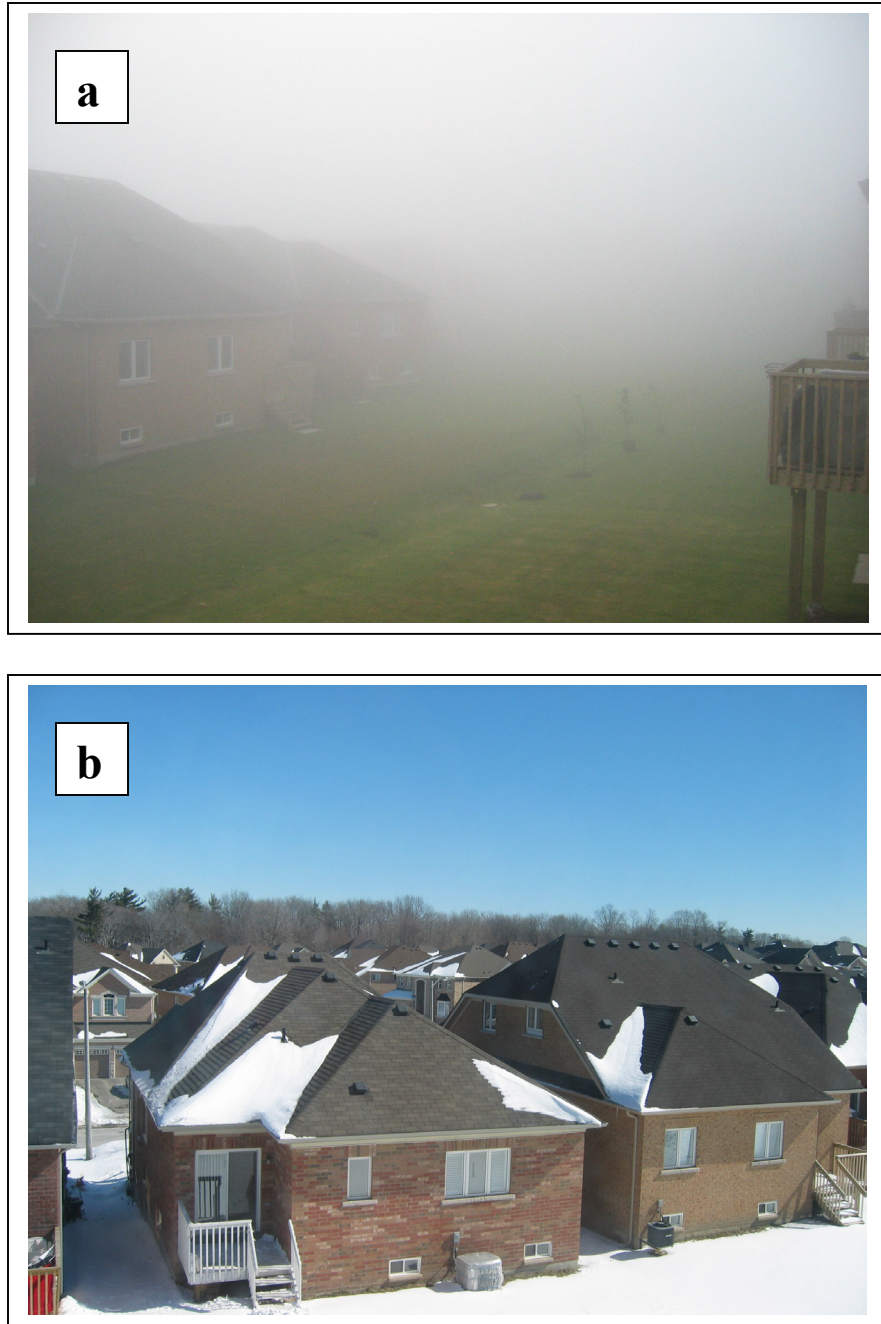


Figure 3: A heavy fog case versus clear air case for a same area. Heavy fog is represented by many small droplets (a), on the other hand, clear air case has a very few or no droplets (b), indicating the importance of droplet number concentration for visibility.

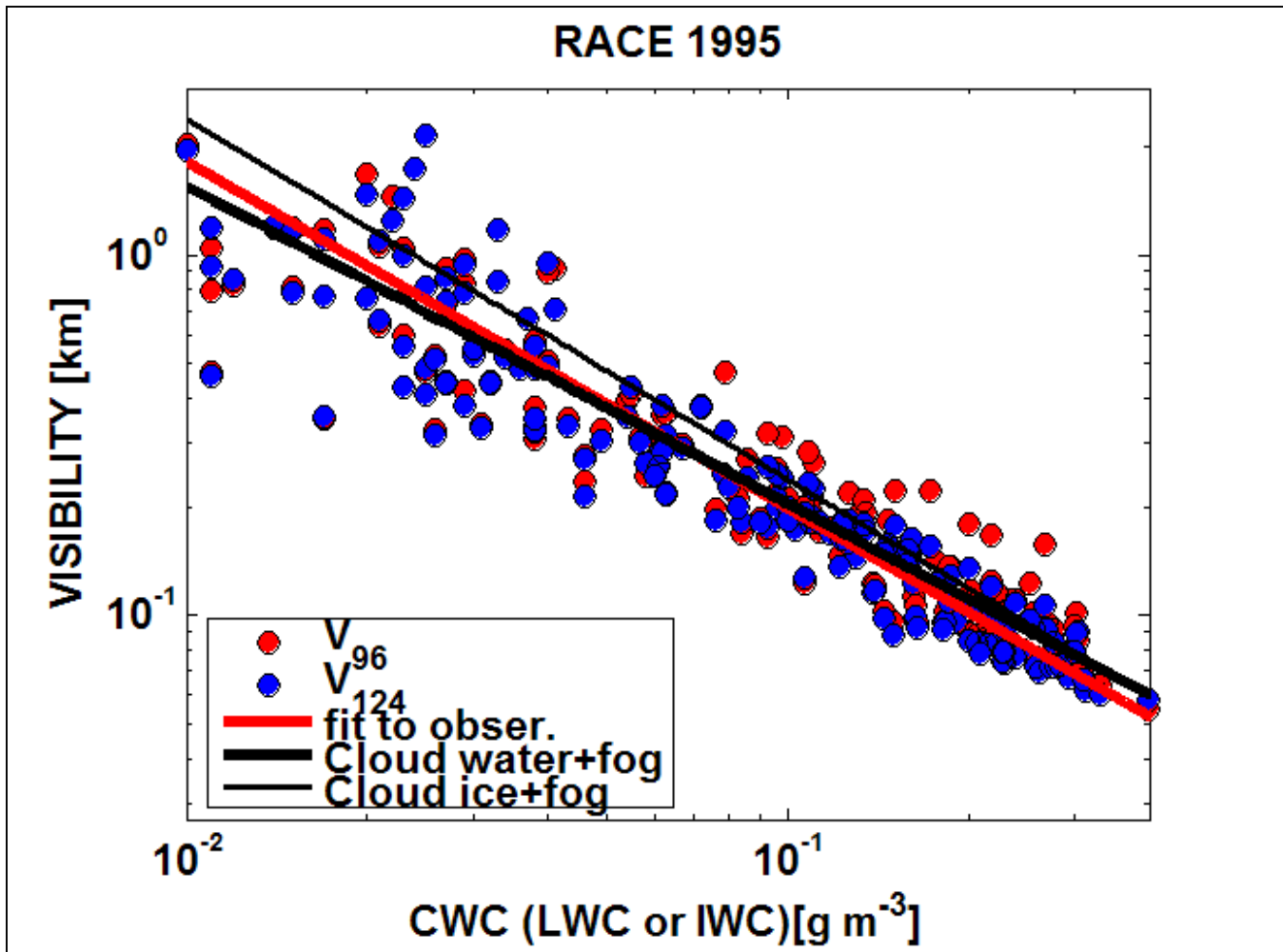


Fig. 4: The visibility calculated from FSSP measurements and Kunkel (1984) versus *LWC* are shown as red line and thick black line, respectively. *IWC* is shown as a reference (thin black line). The red and blue filled circles are for FSSP-96 (over original size ranges) and FSSP-124 (over extended size ranges) observations, respectively.

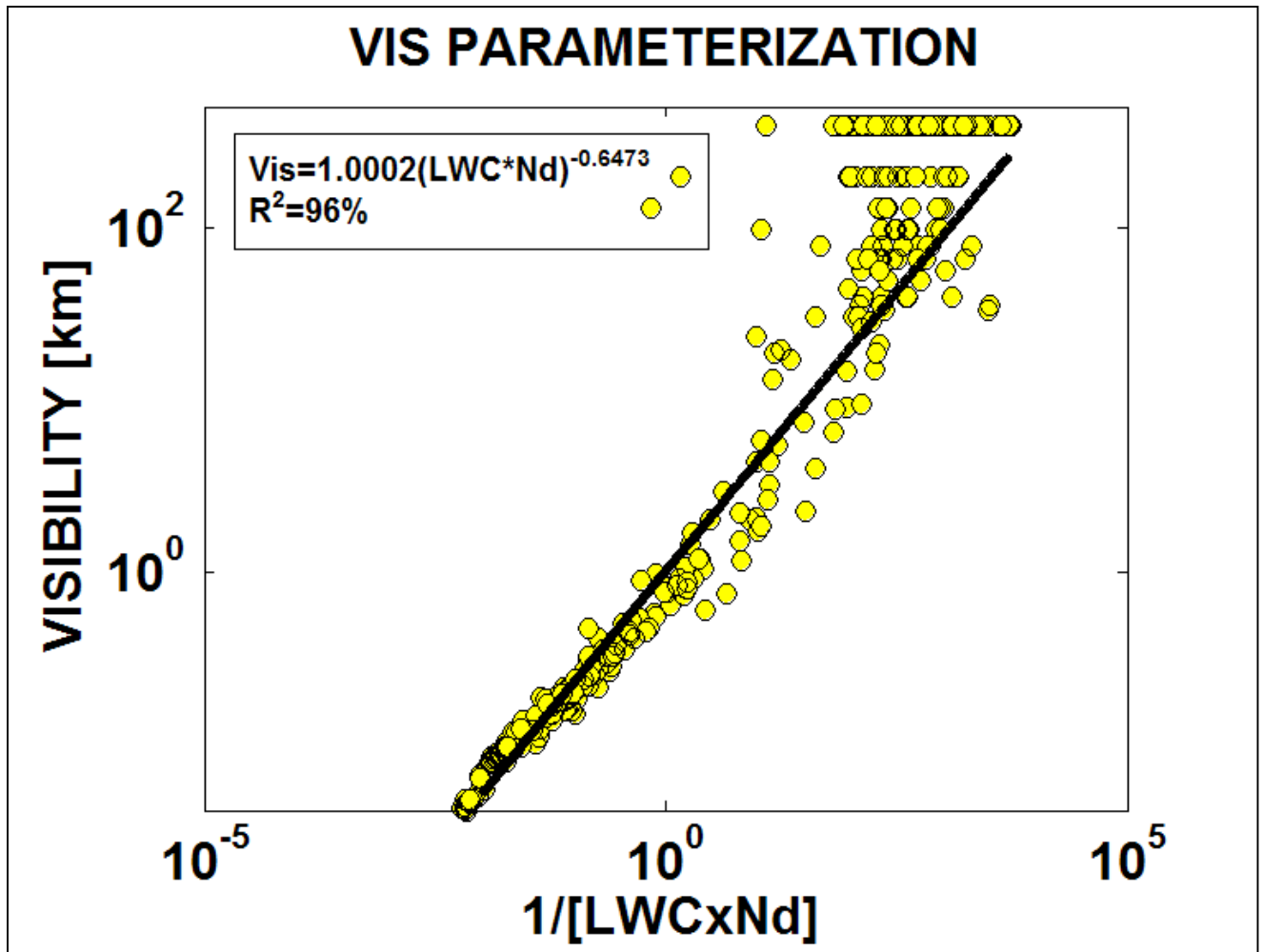


Fig. 5: Visibility versus  $f(LWC, N_d)$  from in-situ observations. The equation for the fit is shown on the figure.

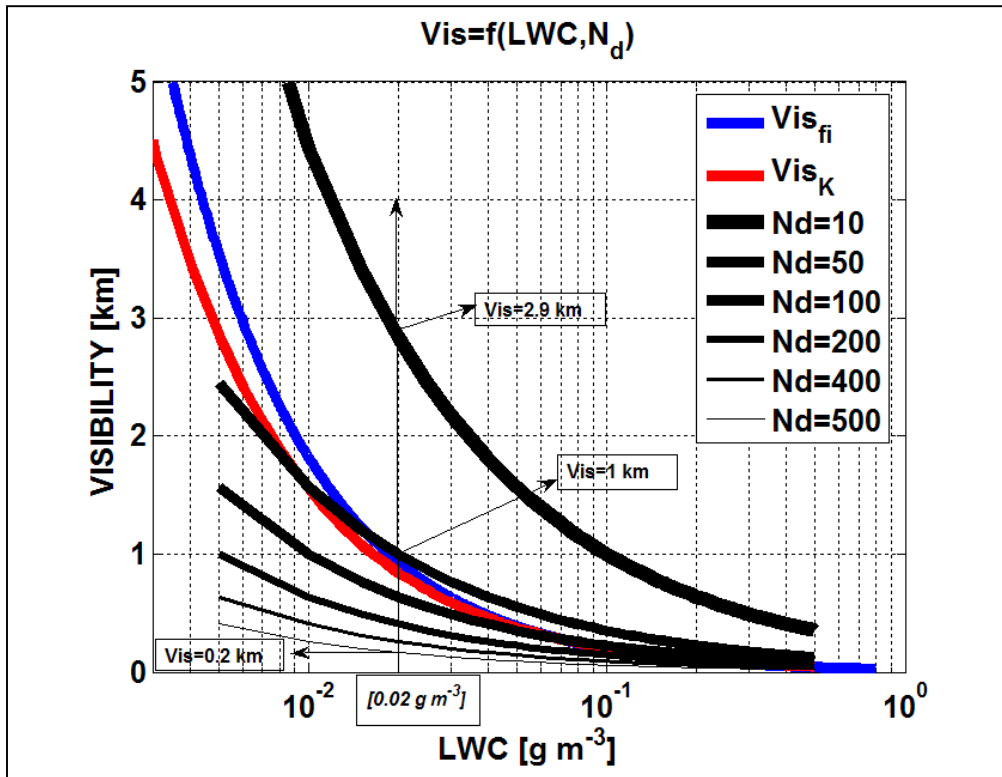


Fig. 6: Visibility versus LWC based on assumed  $N_d$  values corresponding to the observations. The red line is obtained from the Kunkel (1984) work and blue line is from the Eq. 6. The black lines for  $Vis_{fi}$  (Eq. 9) represent the varying  $N_d$  values shown in the panel. The  $Vis$  values within the boxes are for an assumed value of  $LWC$  as  $0.02 \text{ g m}^{-3}$

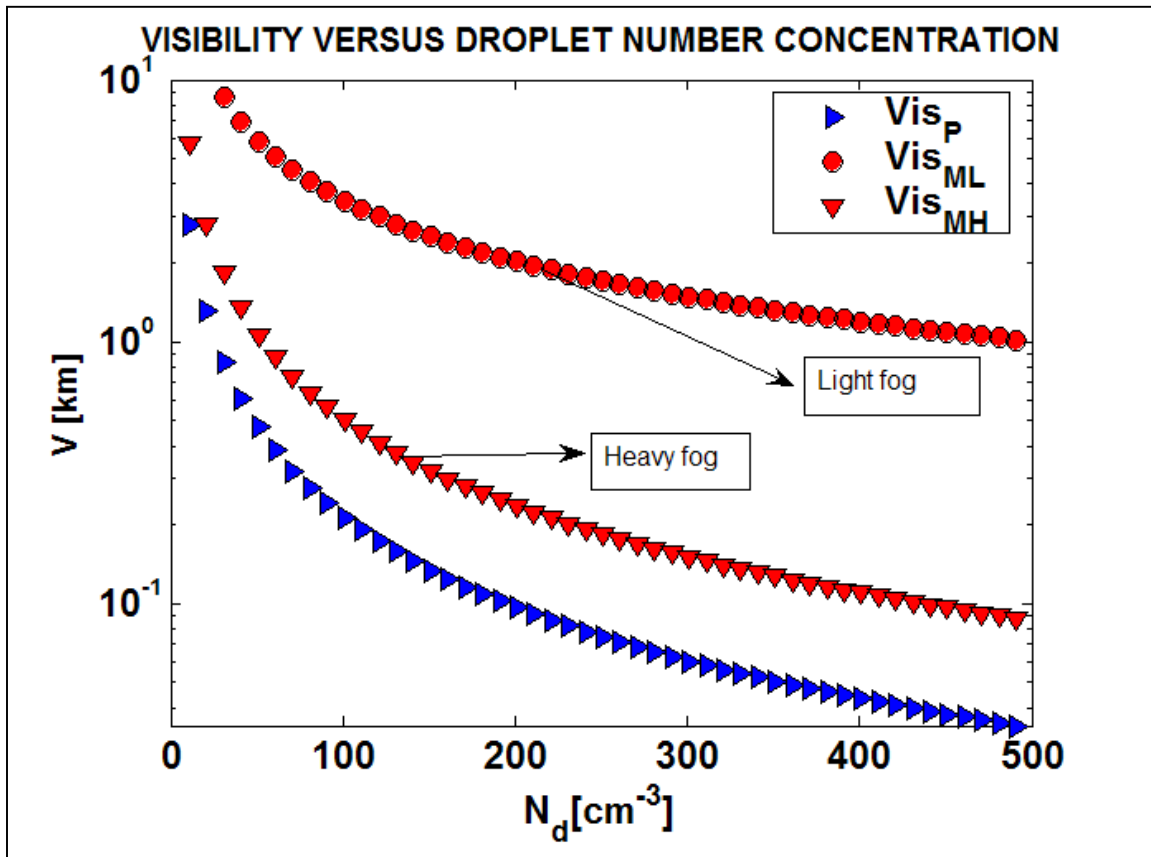


Fig. 7: The visibility ( $Vis_P$ ) as a function of  $N_d$  from the present work and those from Meyer et al. (1980) for light ( $Vis_{ML}$ ) and heavy fog ( $Vis_{MH}$ ) conditions.

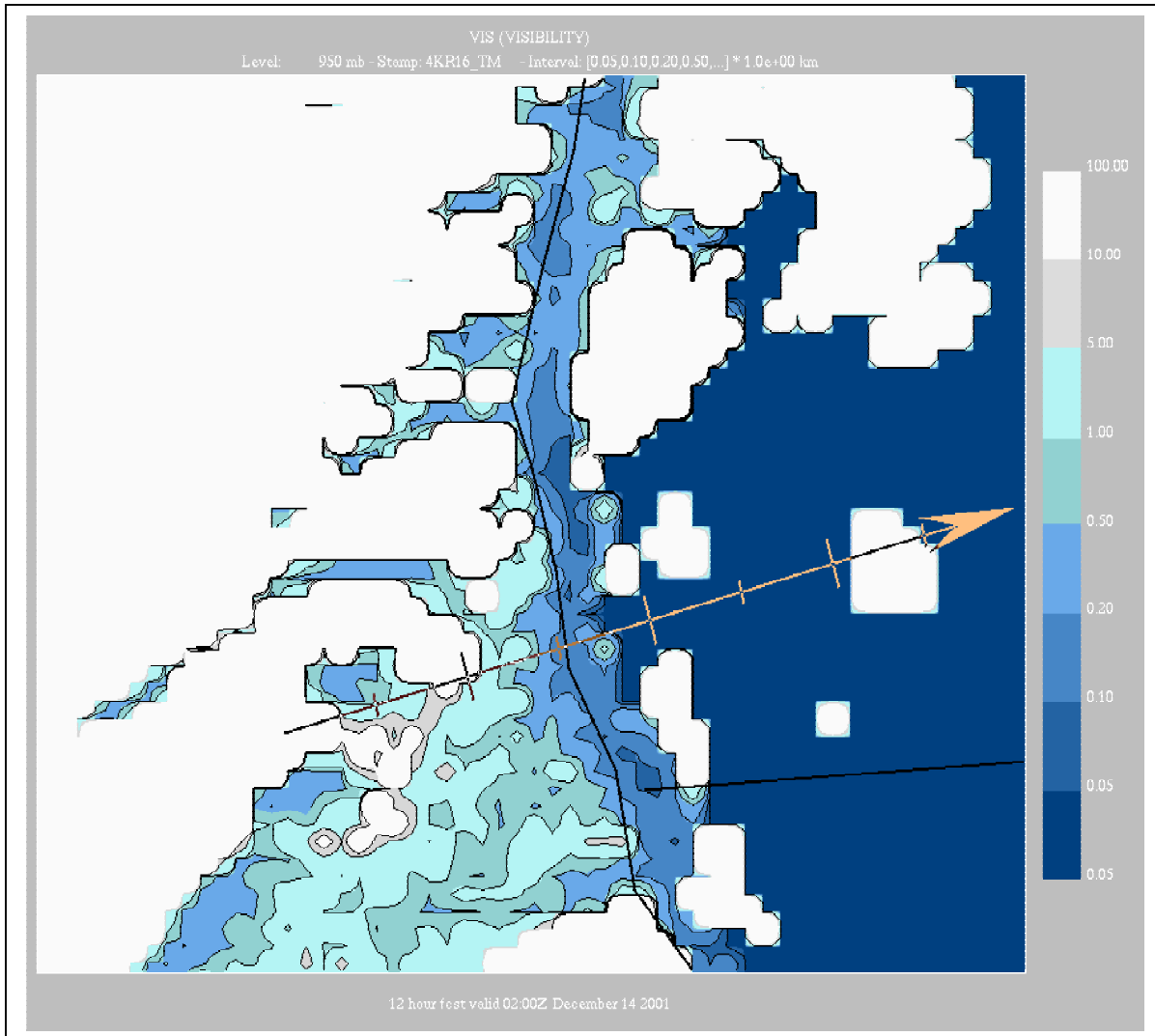


Figure 8: Horizontal view of Vis calculated using the new parameterization (Eq. 9) based on the MC2 model 12-hour forecast valid at 0200 UTC on December 2001. A cross section is taken along the yellow line extends from (42.17N, 234.75W) to (42.56N,236.95W), and the results are shown in Fig. 9. Dark blue color shows Vis < 50 m. Light blue color shows Vis between 1 and 5 km.

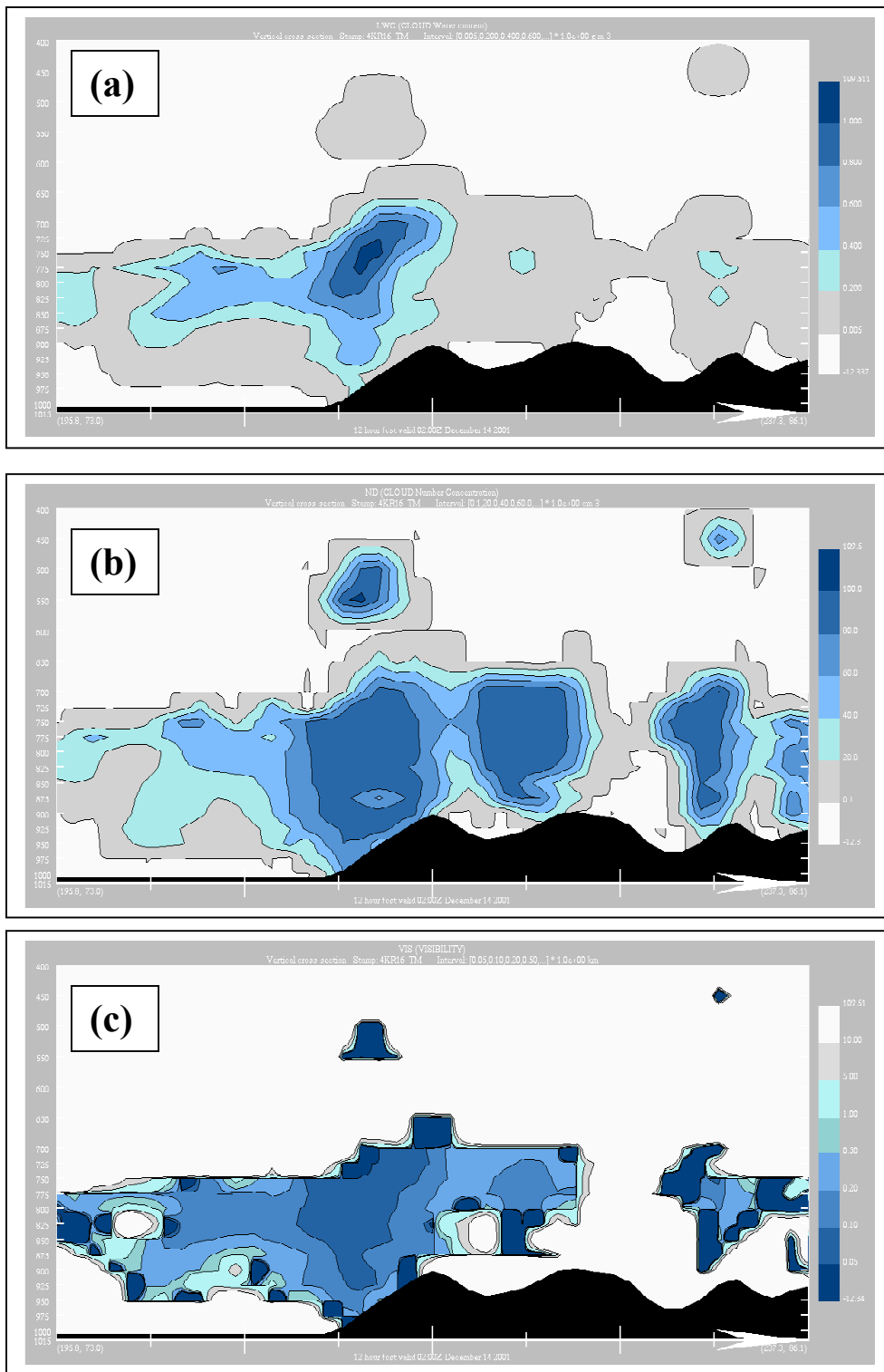


Figure 9: Cross sections of LWC (box a),  $N_d$  (box b), and Vis (box c). Vis values <200 m are seen at western edge of the mountain region. In that location,  $LWC \sim 0.2 \text{ g m}^{-3}$ , and  $N_d \sim 40\text{-}80 \text{ cm}^{-3}$ . These numbers are comparable with observed values shown in Fig. 6.